22A03

The analysis of fast electrons by measurement hard X-ray during current drive by EC waves in QUEST

QUESTにおける電子サイクロトロン波を用いた電流駆動時の硬X線計測と高速電子挙動解析

TASHIMA Saya, ZUSHI Hideki, ISOBE Mitsutaka, IDEI Hiroshi, OKAMURA Syouichi, HANADA Kazuaki, NAKAMURA Kazuo, FUJISAWA Akihide, HASEGAWA Makoto, NAGASHIMA Yoshihiko, ISHIGURO Masaki, KAWASAKI Syouji, NAKASHIMA Hisatoshi, HIGASHIJIMA Aki

田島西夜，図子秀樹，磯部光孝，出射浩，岡村昇一，花田和明，中村一男，藤澤彰英, 長谷川真，永島芳彦，石黒正貴，川崎昌二，中島寿年, 東島亜紀

IGSES, Kyushu University, Kasuga, Fukuoka, 816-8580, Japan

816-8580 福岡県春日市 6-1 九州大学大学院　総合理工学府　先端エネルギー理工学科

To investigate the contribution of fast electron in the non-inductive plasma current (I_p) in electron cyclotron heated (ECH) plasma, the experiment at three magnetic configuration with different vertical field (B_z) curvatures are performed in the QUEST. I_p and flux of the hard X-ray photon (Γ_{HX}) are compared with different magnetic configuration as a function of B_z. In the magnetic field of negative curvature, trapped or stagnation electron are easily losed. In the magnetic field of moderately positive curvature, I_p and Γ_{HX} are respectively fourth and three times lagers than them in the magnetic field of negative curvature at week B_z (< 2 mT). In the strong curvature, I_p and Γ_{HX} are respectively three and ten times lagers than them in the moderately positive curvature, at strong B_z (> 3 mT).

1. Introduction

For steady state operation of tokamak devices, non-inductive current start-up and maintenance are one of the important research fields. Especially ECH has been found to be effective for plasma breakdown and production of a seed current I_{seed} non-inductively. Although three mechanisms of I_{seed} have been proposed in the open magnetic field configuration, the final conclusion is still open.

1)The return current along the spiral field line that cancels the charge separation due to the ∇B drift.

$I_p = 2\langle P\rangle S/RB_z$ (1) , [1]

2) The current by the electrons whose toroidal drift is cancelled by the vertical component of $v_{//}$. [2]

$v_z = v_{//}(B_z/B_t) - m(v_{//}^2 + v_\perp^2/2)/eRB \approx 0$ (2)

3) The toroidal precession current caused by the banana orbits of the trapped electrons.

Here, <P>is spatially averaged plasma pressure, S is cross-section area of plasma current, R is the plasma major radius, B_t is toroidal field. In the CDX-U device, the closed field configuration can be obtained in ECH plasma under steady B_z, and relationship of $I_{seed} \propto B_z^{-1}$ is obtained [3]. This is consistent with first mechanism. In addition, the fact that the particle confinement time in the open field configuration shows the maximum at the optimized B_z has been interpreted on the balance between the parallel loss along the spiral field lines and radial E×B drift loss in WT-2 [4] and TORPEX [5]. In QUEST it has been also observed that I_{seed} agrees with the optimized B_z[6]. In order to discriminate the second and third mechanisms for I_{seed} dependence of the decay indexes $n^* = -d(\mathit{ln}B_z)/d(\mathit{ln}R)$ has been carried out in TST-2 [7]. Results show that I_{seed} is independent of n*. In the present research, to investigate the driven mechanisms of I_p and n* dependence of fast electrons, HX measurement is performed. Both B_z and $n^*$are surveyed. Furthermore how I_{seed} is increased with increasing B_z and connects the driven current I_p are investigated.

2. Device and experimental conditions

QUEST is a medium sized spherical tokamak device [8]. B_z can be produced by a three sets of Poroidal field coils PFs, PF17, PF26, and PF35. n* is -0.2(PF17), 0.25(PF26) and 0.5 (PF35) at (R,Z)=(0.6 m ,0 m), respectively. The O-mode waves with parallel refractive index N|| of 0.4 are injected from the low field side via a phased array antenna. In the present experiments the resonance position is fixed at R=0.3 m. HX flux (Γ_{HX}) is horizontally detected by the semiconductors. The pulse height analysis for the photon flux in the energy range of < 400 keV is done at the dwell time of 1-5 ms.

Two cases of experiments are conducted. For the case 1, production of I_{seed} is investigated at low power P_{rf} of 17 kW and constant B_z in time. Three PFs configurations are used, time averaged current

<I_{seed}> is used. I_{seed} and Γ_{HX} are studied as a function of B_z and n*. For the case 2 ramp-up of I_{seed} and Γ_{HX} is studied with temporally increasing B_z and then a relation between I_p and B_z is compared with the conventional tokamak equilibrium. In order to ramp-up I_p P_{rf} is raised up to 40 kW.

3. Experimental results

Figure 1 shows the B_z dependence of <I_{seed}>and Γ_{HX} for the PF17 and PF26 configurations. For the former, no current is generated for B_z < 0.8 mT, <I_{seed}> is ~ 1 kA at B_z ~ 1.0 mT and decays for B_z > 1 mT. For the latter, <I_{seed}> increases linearly up to 4 kA with B_z of 1.6 mT , but <I_{seed}> cannot be created avove 1.6 mT. Thus, the clear n* dependence on <I_{seed} >is confirmed. Γ_{HX} is not observed for B_z < 0.8 mT, but appears for B_z> 0.8 mT for both cases. For the PF17 case Γ_{HX} peaks at B_z of 1.2 mT, but Γ_{HX} for the PF26 case peaks at slightly higher B_z of 1.5 mT. At the higher B_z Γ_{HX} is reduced, but a finite intensity is observed though <I_{seed}> is < 1 kA.

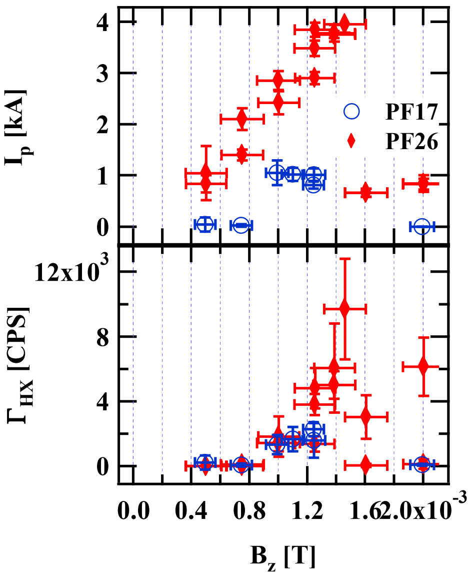

Fig. 1 Time averaged I_p and Γ_{HX} function of B_z.
♦; PF26coil configuration○; PF17coil configuration

Figure 2 shows the comparison of B_z dependence of <I_p> for the PF35 case, with those of the PF26 case. Although both the maximum of <I_p> are ~ 5-6 kA, the relation with B_z is quite difference. For the PF35 case the maximum value of <I_p> is obtained at B_z of 8 mT, while no current is generated for the PF26 case for B_z>1.6 mT. In order to increase I_p for the PF 26 case the B_z ramp-up scenario (the case 2) must be used, as denoted by open diamonds in the Figure 2. For the PF35 case, when P_{rf} > 60 kW, more than 10 kA can be easily accessed without ramping–up B_z. Therefore, the confinement of the energetic electrons and generation mechanisms of I_{seed} seem to be strongly dependent on n* from 0.25 to 0.5.

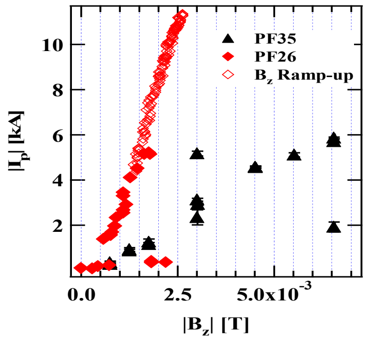

Fig. 2 Time averaged I_p function of B_z. ♦ ; PF26coil configuration with constantly B_z. ▲; PF35coil configuration with constantly B_z ◊ ; B_z ramp-up

For PF 35 case Γ_{HX} 1.8 times greater than in PF26 case at B_z = 3 mT, and trend of Γ_{HX} is same as I_p.

4. Discussion and Summary

In order to investigate the electron confinement in these magnetic configurations, the electron orbits, which are launched at the vessel center (R = 0.6 m and z = 0 m), are numerically investigated for the energy range from 1 keV to 30 keV, at various pitch angles. In the PF17 case, all electrons are lost at the wall, because no trapped particles can be allowed. Therefore the B_z dependence of <T_{seed}> and orbit calculations suggest that the first mechanism may play a role for current generation.

The equilibrium B_z is estimated by eq. (3)

$$B_z = \frac{\mu_0 I_p}{4\pi R}(In\frac{8R}{a} + \frac{l_i}{2} - \frac{3}{2} + \beta_p) \quad (3)$$

Here, $\beta_p = 8\pi^2 a^2 <P>/\mu_0 I_p^2$, $<P> = n_e T_e$, T_e is the electron temperature (~100 eV), n_e is the electron density (~1×10^{17} m^{-3}). For the PF 26 case, the relation indicates a conventional low β_p equilibrium. However, for PF35 case, the larger B_z is required for higher β_p. The role of the energetic electrons on β_p is essential.

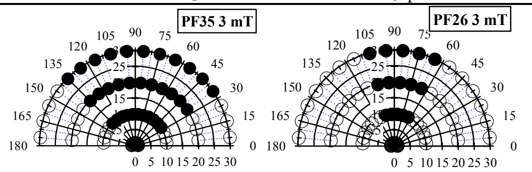

Fig. 3 The confined areas in the velocity space
○;Lost ●;confined

References

[1] L. E. Zakharov, et al., Plasma Phys. **14**, 75 (1988)
[2] J. Sugiyama, A. Ejiri, et al., Plasma and Fusion
[3] C.B. Forest, et al., Phy. Rev. Lett. **68** (1992) 3559
[4] S. Nakao et al., Phys. Lett. **96**A (1983) 405
[5] S.H.Muller, et al., Phy. Rev. Lett. **93** (2004) 165003
[6] J. Sugiyama, A. Ejiri, et al., Plasma and Fusion
[7] S. Tashima, H. Zushi, et al., Journal of Plasma and Fuion Research **9**(2010) 316]
[8] K. Hanada et al., 22nd IAEA FEC FT/P3-25,2008
Res. Letters **3**, 026 (2008)
[9]T. Yoshinaga, et al., PRL **96**, 125005 (2006)